Chapter 2

Science

The Auger Project will explore the cosmic ray energy spectrum and arrival direction distribution above 10^{19} eV as a function of the mass of the primaries. Such data will shed light on the origin of these cosmic rays, on the distance of the sources, and on the magnetic field structure and strength between the sources and the earth. Further, for the subset of particles whose types have been identified, it may be possible to obtain information of relevance to particle physics at energies well beyond those ever attainable in terrestrial accelerators.

This chapter surveys the astrophysics and cosmology which underlies current thinking on the origin of the highest energy cosmic rays. It has proven difficult to construct a satisfactory theory. The fundamental obstacle to understanding the nature of these particles is the lack of data; the next chapter summarizes the present observational status. Here, we begin by discussing general principles of acceleration and propagation of extremely energetic particles, highlighting significant constraints on the possible sources. Next, we review some recent theoretical work. We conclude the chapter by describing the kind of measurements which are required to test theories.

2.1 Introduction

A detailed measurement of the energy spectrum will yield a wealth of important information on the nature of the highest energy cosmic rays. Soon after the discovery by Penzias and Wilson [11] of the cosmic microwave background radiation (CMBR), Greisen [12] and Zatsepin and Kuz'min [13] independently pointed out that this radiation would make the universe opaque to cosmic rays of sufficiently high energy. This occurs, for example, for protons when their energy exceeds the threshold for pion photoproduction (via the Δ^+ resonance) in an encounter with a photon of the CMBR. The reaction sequence $p\gamma \rightarrow \Delta^+ \rightarrow \pi^\circ p$ effectively degrades the energy of the proton. The characteristic attenuation length is less than 50 Mpc[1] when the proton's energy is greater than 10^{20} eV. A similar phenomenon of

[1]50 megaparsecs (Mpc) is the distance light travels in 150 million years. The center of the Virgo cluster of galaxies, of which our own Milky Way is a member, is approximately 20 Mpc away.

energy degradation also occurs for nuclei due to processes of photodisintegration. This is a small fraction of the size of the Universe and has the following implications:

- If the highest energy cosmic rays are universal in origin, then the observed energy spectrum should not extend, except at greatly reduced intensity, beyond about 5×10^{19} eV, a phenomenon known as the Greisen-Zatsepin-Kuz'min (GZK) cut-off.

- Particles with energy above the GZK cut-off must come from nearby, cosmologically speaking. Over modest distances, charged particles of such high energy would traverse cosmic magnetic fields with little deviation. Their observed trajectories would thus indicate the direction to their sources. It may therefore be possible to identify the sources of these particles with previously known astrophysical objects, or else to establish the existence of new sources which are not visible at lower energies. Identification of such sources requires that many cosmic ray events are detected from each one.

Due to their extremely low flux, the study of cosmic rays above 10^{19} eV requires extremely large detectors. This is illustrated in Figure 2.1, which shows a recent compilation[14] of measurements of the cosmic ray differential energy spectrum. The dotted line represents an E^{-3} spectrum for comparison. Also indicated are approximate integral fluxes (per steradian) above certain energies where the spectrum shows changes in its power law behavior. The observed rate of events above 10^{19} eV is about 0.5 events/km^2/year/steradian; above 10^{20} eV, the rate has diminished by roughly a factor of 100.

Such large areas are, for the foreseeable future, only possible with ground-based air shower detectors. Current experiments, with areas of order 100 km^2, are limited in the number of events they can collect in the crucial energy region above 10^{19} eV. While there is insufficient data to answer the fundamental questions, present results hint at several interesting and important phenomena. For example, a recent analysis of a subset of the available data[15] noted that there were 7 events observed with energies exceeding 10^{20} eV, while a simple power-law extrapolation of the experiments' observed spectra at lower energy predicts more than 20. Since there is also the suggestion of a slight flattening of the spectrum above 10^{19} eV, these observations may be indicating interesting spectral structure. Could this be evidence for the GZK cut-off? On the other hand, there definitely are several events with $E > 10^{20}$ eV, which must originate from relatively nearby. What are their sources?

These questions will be discussed in more detail in the next chapter. To summarize, there simply are not enough data above 10^{20} eV to draw definitive conclusions. The Auger Project is designed to remedy this problem.

Much new theoretical work has already been stimulated by the recent observation of two events with estimated energies $E \geq 2 \times 10^{20}$ eV [4, 6] and also by the series of workshops on the Auger Project. None of the theories proposed to date accounts for all the facts in a really satisfactory way. The present data raise questions of great importance for astrophysics, cosmology, and fundamental physics.

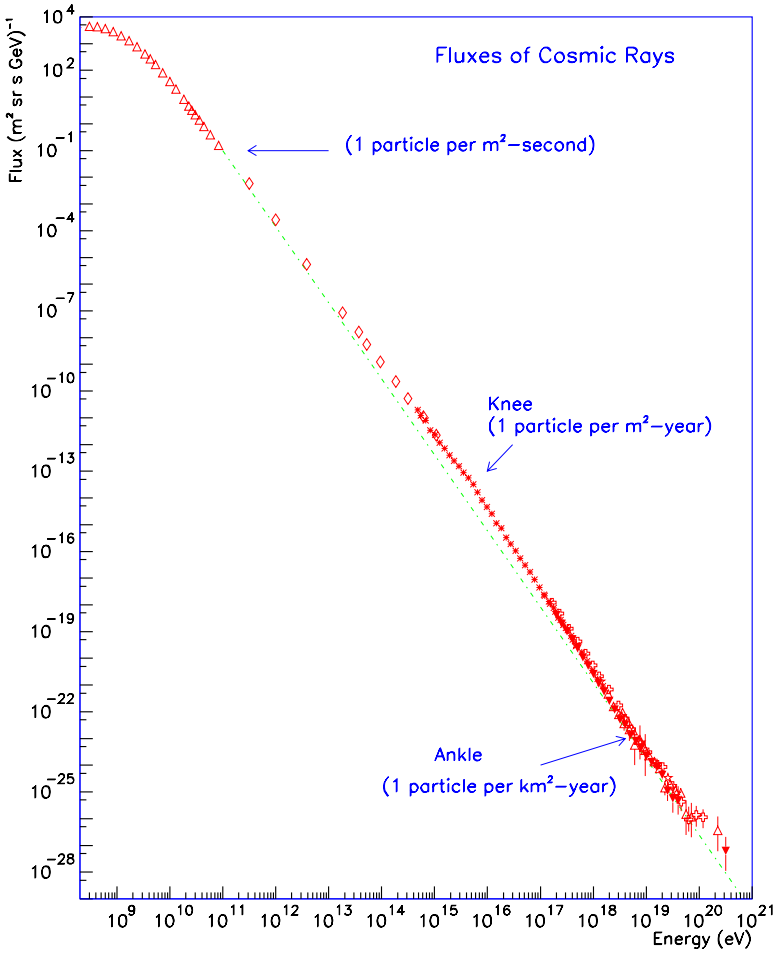

Figure 2.1: Compilation[14] of measurements of the differential energy spectrum of cosmic rays. The dotted line shows an E^{-3} power-law for comparison. Approximate integral fluxes (per steradian) are also shown.

2.2 Acceleration and propagation of cosmic rays

The two central questions about the highest energy cosmic rays are how, and where, they are accelerated. The most energetic particle yet detected, presumably a single proton or a nucleus, had a macroscopic energy of 50 joules — roughly the kinetic energy of a tennis ball at 100 mph! Its energy, 3×10^{20} eV, is more than eight orders of magnitude higher than can be achieved by the most powerful man-made accelerator. Over the years a few events with energies near 10^{20} eV have been recorded. More recently two events have been observed with energies well above the GZK cut-off and have, as a result, attracted significant attention and scrutiny. Each of the groups involved has devoted a paper to a critical review of the events and the analysis leading to their energy assignment [4, 6]. As will be shown, because of the limited range and high magnetic rigidity of such particles, a detector with sufficient collecting power will be able to determine their sources.

2.2.1 Acceleration

Acceleration in astrophysical settings occurs when energy in large-scale macroscopic motion is transferred to individual particles[17]. The macroscopic motion could, for example, be associated with turbulence or shock waves in plasmas. Another scenario is the environment near a rapidly spinning, magnetized compact object. There are also more speculative models invoking exotic mechanisms, such as topological defects.

Fermi acceleration

In 1949, Fermi[18] developed a model where particles can achieve high energies through repeated encounters with moving, magnetized plasmas. This process ("Fermi acceleration") is often referred to as stochastic or diffusive acceleration, since high energies result from particles randomly scattering many times within a confined region, with some chance of escaping the region permanently. The magnetic field, B, embedded in the plasma plays a crucial role.

Fermi demonstrated that the geometry of moving plasma clouds is such that the *average* energy change per encounter is positive and proportional to the particle's energy: $\Delta E = \alpha E$. After k encounters, a particle initially with energy $E_\circ$ will achieve an energy $E = E_\circ(1+\alpha)^k$. Suppose P_{esc} is the probability per encounter that the particle escapes the containment region and is no longer accelerated. The number of particles which survive long enough to reach some energy E is given, by summing over k, to be $N(> E) \propto E^{-\gamma}$, where $\gamma \approx P_{esc}/\alpha$, if P_{esc} and α are each small. Thus, Fermi acceleration naturally produces a power-law spectrum of particle energies.

Fermi acceleration by astrophysical shock waves is an attractive paradigm with which to construct models of cosmic rays. As shown in Figure 2.1, cosmic rays exhibit a non-thermal power law energy spectrum. It can be shown [17] that the spectral index γ of the Fermi acceleration integral energy spectrum, in the limit of strong shocks, has a value

slightly greater than $\gamma \approx 1$, and is not very dependent upon the details of the environment. Because the particles will undergo energy dependent processes during transport to Earth, the observed spectrum is expected to be steeper than that at production. The experimentally observed integral spectrum varies from $E^{-1.1}$ to $E^{-2.1}$ in various energy regimes, so the predictions of Fermi acceleration are in reasonable accord with data. In situations where Fermi acceleration may occur from plasma motions which are not strong shocks, the spectral index is very sensitive to geometric details and can be quite large.

Perhaps most importantly, Fermi acceleration has actually been observed to occur in the heliosphere (although at much lower energy). One example is the direct observation by the *ISEE* satellite of the acceleration of $\sim 10 - 100$ keV protons by shocks in the solar wind. The data agree in detail with the predictions of Fermi acceleration theory[19].

In general, the maximum possible energy is determined by the length of time over which the particles are able to interact with the plasma. In some cases, the accelerating region itself only exists for a limited time, such as in the case of supernovae shock waves which dissipate after about 10^3 years. Otherwise, if the plasma disturbances persist for much longer periods, the maximum energy may be limited by an increased likelihood of escape from the region. The latter case is relevant to the extreme energies seen in cosmic rays. As particles reach extreme energy, it becomes very difficult to confine them magnetically to the acceleration region.

The simplest modeling[17, 20, 21] of Fermi acceleration by shock waves gives the maximum energy acquired by a particle of charge Ze :

$$E_{max} \approx \beta c \times Z\, e \times B \times L, \tag{2.1}$$

where L is the characteristic size of the acceleration region and βc is the shock velocity ($\beta \approx 0.01$ for supernovae). However, under certain configurations of the shock and the embedded magnetic field, β is replaced by a much larger factor, of order 1-3 [17, 22]. Equation 2.1 essentially states that the gyro-radius of the particle being accelerated must be contained within the acceleration region, as in a terrestrial accelerator. Realistically, it is unreasonable to assume that astrophysical accelerators will have the nearly 100% efficiency required to achieve energies like those in Eq. 2.1; it is more likely that the above value of E_{max} should be reduced by perhaps a factor of ten, depending on the details of the shock and its environment[20].

Figure 2.2 shows where some potential astrophysical accelerators lie in the B–L plane [23]. Objects below the diagonal lines derived from Eq. 2.1 cannot accelerate particles to 10^{20} eV by shock acceleration. The dashed line is for iron nuclei and the solid line for protons, each case for $\beta = 1$. A value of $\beta = 1$ is unrealistically extreme. The top of the shaded region is for protons assuming $\beta = 1/300$, a more typical value for many astrophysical shocks.

It is striking that the most energetic accelerators in the figure appear to have a maximum energy just in the range where the GZK cut-off comes into play. In addition, since for any given configuration of magnetic fields and plasma motion, the maximum total energy for nuclei is approximately Z times higher than that for protons, we expect the observed mass spectrum to have interesting and revealing structure in the energy range above 10^{19} eV.

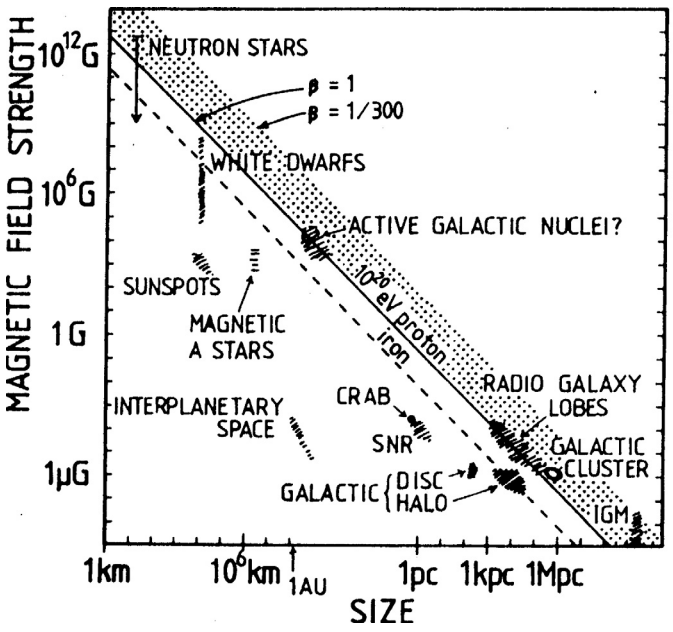

Figure 2.2: Size and magnetic field strength of possible sites of particle acceleration [23]. Objects below the diagonal lines cannot accelerate particles to 10^{20} eV by shock acceleration. Dashed line is for iron nuclei, solid for protons, each with $\beta = 1$. The top of the shaded region is for protons and $\beta = 1/300$. IGM refers to the intergalactic medium; Galactic Cluster refers to accretion shocks in clusters.

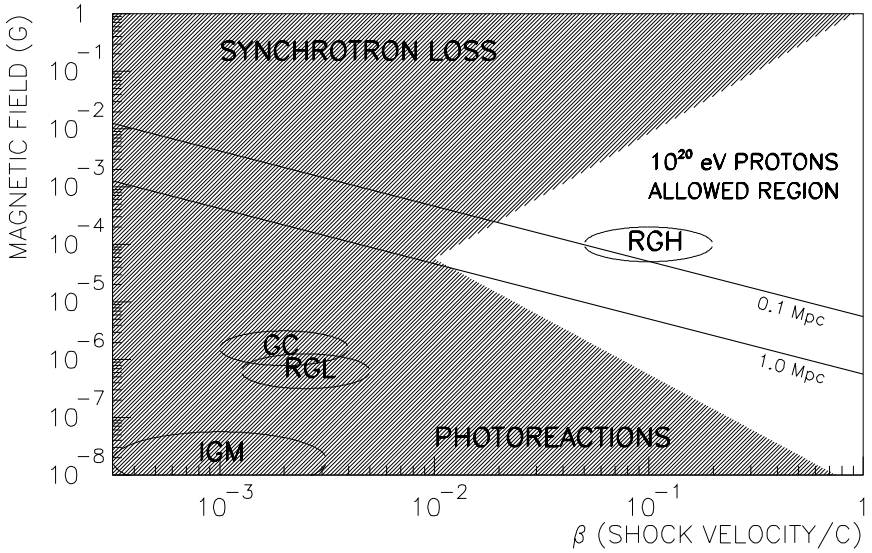

Figure 2.3: Magnetic field strength and shock velocity of possible sites of acceleration (adapted from [23, 24]). Only the unshaded region allows acceleration of protons to 10^{20} eV. Candidate accelerators must also lie above lines appropriate to their characteristic size. Notations are as in the last figure: GC is Galactic Cluster, RGL is Radio Galaxy Lobes. RGH is a subclass of radio-lobe sites added here, denoting radio galaxy hot-spots.

Good energy resolution and sensitivity to the mass of the initiating primary will be required in order, for example, to distinguish between a GZK cut-off for a proton source and the maximum energy of an accelerator for which $E_{max} \propto Z \times e$.

Only a few of the objects in Figure 2.2 appear able to generate particle energies above 10^{20} eV. Generally, large structures associated with galaxies or groups of galaxies seem to have sufficient size and field strength to merit consideration as acceleration sites. Not shown in this figure is a recent suggestion by Cesarsky[25, 26] that the environs of colliding galaxies might also have the appropriate conditions to accelerate particles beyond 10^{20} eV through diffusive shock processes. The magnetic fields will be amplified during the collision above the single galaxy value.

It is often impossible to achieve the maximum energy suggested by Eq. 2.1 and Fig. 2.2. This occurs when conditions are such that the energy loss rate exceeds the acceleration rate. One source of losses is synchrotron radiation, which can become important even for protons at very high energy in regions of extreme magnetic fields. Other loss processes include photoproduction interactions (e.g., $p\gamma \rightarrow \pi^+ n$). These loss rates can dominate all others in compact volumes with intense thermal radiation. It can also be important in large regions of space if the acceleration occurs over long time scales. In the latter case it is the cosmic microwave background radiation that provides the target photon field; indeed, this is the mechanism of the GZK cut-off mentioned earlier.

The effects of synchrotron radiation or interactions with the cosmic background radiation were not included in Figure 2.2. Acceleration ceases when the rate of such losses exceeds the rate at which energy is gained through shock encounters. Figure 2.3 illustrates an estimate of this effect[23, 24], showing that certain combinations of shock velocity and magnetic field strength can prevent the acceleration process from achieving energies as high as 10^{20} eV. An estimate of the allowed region of $B - \beta$ space was made as follows. The rate of energy gain from shock acceleration is parametrized as $dE/dt \propto \beta^2 B$, by replacing L in Eq. 2.1 by βcT (with T some characteristic time over which the shock acceleration process works), and differentiating. Equating this rate with that of losses from synchrotron radiation ($dE/dt \propto B^2$) or photoreactions ($dE/dt \approx$constant), one obtains the diagonal boundaries of the disallowed regions in the Figure 2.3. Note that this calculation was done for photoreactions on the cosmic background radiation; even more of $B - \beta$ space would be excluded if the target radiation field was the intense, higher energy environment near an AGN. It can be seen here that the rate of energy gain from most of the potential accelerators in the Figure 2.2 is too slow to overcome losses due to photoreactions.

Compact objects

Compact objects with very large magnetic fields, such as neutron stars or Active Galactic Nuclei (AGNs), also appear in Figure 2.2 near the diagonal lines which indicate the requirements for shock acceleration to 10^{20} eV. However, in these compact systems, shock acceleration (perhaps in accretion flows) is not the only means to accelerate particles. The rapid rotation of small, highly magnetized objects generates enormous electric fields. These fields might then accelerate particles in so-called "one-shot" mechanisms. It turns out that

the upper limit on the energy in such models is given by a formula quite similar to the shock acceleration case in Equation 2.1 [27]. For example, the maximum energy available from a rotating neutron star can be obtained by dimensional analysis as $E_{max} = eZ\omega B_s R_s^2/c$ where ω is the pulsar angular velocity, B_s a surface magnetic field and R_s the neutron star radius. Representative values of $B = B_s$ and $L = R_s$ for neutron stars were shown in Fig. 2.2, and the combinations required to achieve 10^{20} eV energies would lie on a line very similar to that shown for the shock wave case.

When realistic models of acceleration are constructed, however, this ideal dimensional limit for neutron stars is not realized [27]. For example, in an aligned rotator, the maximum potential available is the integral of the electric field from the pole to the last open field line which extends beyond the light cylinder. In this case the dimensional estimate of E_{max} is reduced by an additional factor of $\omega R_s/c \leq 0.1$. Further, it is generally true that the energetic particles which may be produced will suffer significant degradation of their energy in the intense local radiation fields. Examples include curvature radiation near neutron stars or photodisintegration of nuclei and photopion production by protons near the cores of AGN.

Nevertheless, it may be possible to have field geometries associated with compact objects which are able to accelerate particles to extreme energy. Colgate has described one scenario where electrostatic fields are aligned with magnetic flux surfaces[28]. This configuration arises during reconnection of magnetic fields in plasmas. Pulsars or AGN at the cores of quasars may be examples. In Colgate's model, a single traversal by a charged particle of a reconnection surface associated with the twisted flux surfaces extending from a quasar accretion disk to the radio lobes can lead to particle energies well above those presently observed.

Exotic accelerators

Inspection of Figures 2.2 and 2.3 suggests that few of the proposed astrophysical accelerators can easily account for energies as high as 10^{20} eV. Indeed, the possibility exists that the very highest energy particles come not from these "conventional" objects but are produced directly by some exotic mechanism (e.g. the so-called "topological defects"). Such sources could produce jets of hadrons and photons with energies well above 10^{20} eV that would then cascade down to lower energy. This particular scenario has its own potential difficulties, which will be mentioned in a later section. Nevertheless it is clear that cosmic rays in this energy range have the potential to teach us about particle physics far beyond the reach of even dreamt-of accelerators.

2.2.2 Propagation and the GZK Cutoff

Cosmic ray particles do not travel unhindered through space. They are subject to various interactions and their trajectories may be curved by magnetic fields. The result of these effects will characteristically alter the observed energy spectrum and arrival directions at earth.

For a cosmic ray nucleus of charge Ze in a magnetic field $B_{\mu G}$ in μGauss, the Larmor radius in kiloparsecs (kpc) is

$$R_{kpc} \approx E_{18}/(Z\, B_{\mu G}), \tag{2.2}$$

where E_{18} is the total energy of the particle in units of 10^{18} eV. Since the disk of the Galaxy is significantly thinner than 1 kpc, and magnetic fields there are on the order of a few μGauss, if all cosmic rays are from sources in the disk, they must exhibit a tendency to come from the galactic plane at higher energies. At present there is no statistically significant evidence for cosmic ray arrival directions to cluster along the Galactic plane. It is therefore reasonable to assume that particles with $E > 10^{19}$ eV are extragalactic in origin, even for heavy particles such as Iron nuclei ($Z = 26$). (Indeed, it has been proposed that if nuclei can be identified with a specific source direction, then it may be possible to use the large-scale magnetic field in the disk of the Galaxy as a magnetic analyzer, correlating deflections with energy and charge. This will be discussed in the next chapter.)

If cosmic rays seen at earth have an extragalactic origin then they have survived a very long time. There are several processes that can degrade the energy of particles as they propagate through the cosmos [17]. We have already mentioned one mechanism whereby protons produce secondary hadrons in interactions with the microwave background. They may also lose energy through the production of electron-positron pairs in the background radiation. After pion photoproduction, the proton (or perhaps, instead, a neutron) emerges with a reduced but still very large energy. Further interactions occur until its energy is below the GZK cut off[29].

Nuclei also undergo photo-disintegration in the CMBR and infrared radiations[30], losing about 3-4 nucleons per Mpc traveled when their energy exceeds about 2×10^{19} eV[31]. Although the latter process occurs at a lower energy per nucleon than pion photoproduction by protons, the thresholds for the two processes are nearly the same when expressed in terms of the total energy of the nucleus. Hence, no nucleus can be observed at earth with such energy if the source is more than about 20 Mpc distant.

The attenuation lengths for these processes are shown in Figure 2.4. Also shown is the interaction length of high energy photons which interact with various background radiations and produce electron-positron pairs[29]. In this case we show separately the attenuation of photons in diffuse infra-red radiation, the radio background, and the CMBR. The radio and infra-red backgrounds are, however, much less well determined than the microwave radiation.

Note the line in Figure 2.4 marked "red shift limit". All particles lose energy over time due to the general expansion of the universe. The time scale over which a particle would suffer complete energy loss from this effect is of order

$$\tau_H = (\frac{1}{E}\frac{dE}{dt})^{-1} \approx H^{-1},$$

where H is the Hubble constant. The constant $c\tau_H$ is plotted in this figure, representing an absolute upper limit on the distance a particle can travel before expiring.

As a consequence of the various background radiation fields, there are limits to how far away the sources of extremely energetic particles can be, no matter how high their initial

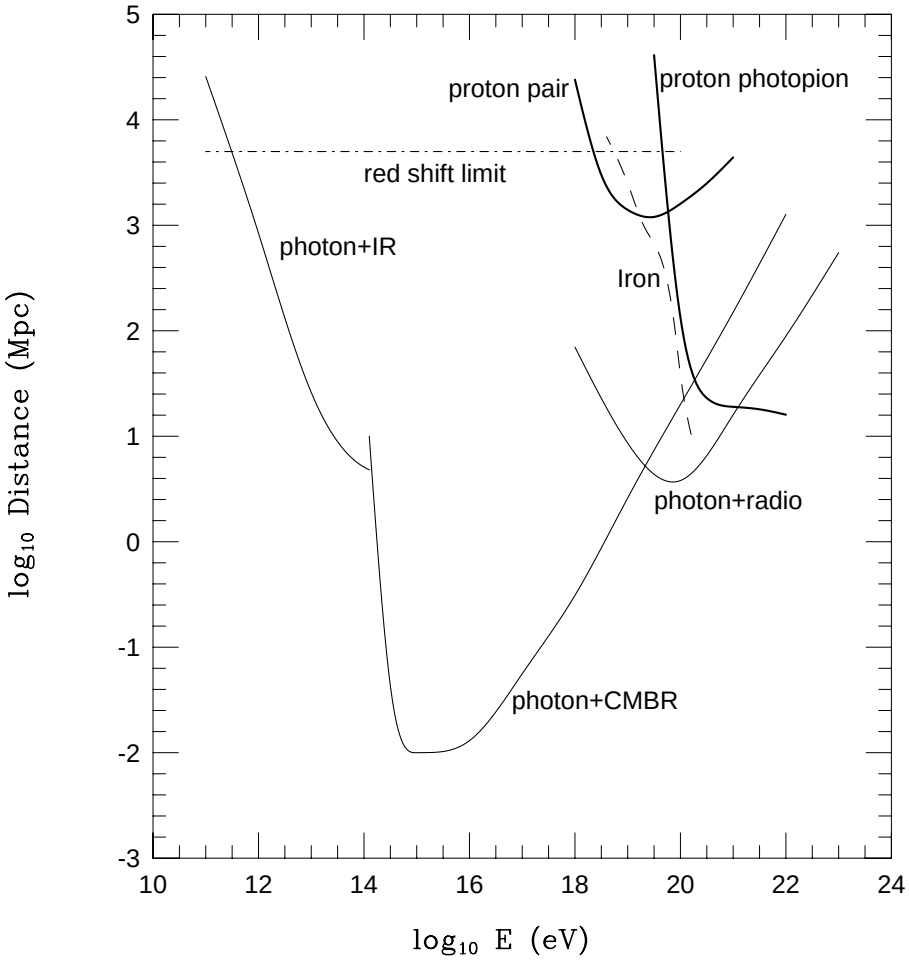

Figure 2.4: Attenuation length of photons, protons and iron in various background radiations as a function of energy. The three lowest and left-most curves refer to photons, showing the attenuation by infra-red, microwave background and radio [29]. The upper, right-most solid curves refer to propagation of protons in the microwave background, showing separately the effect of pair production and photo-pion production [29]. The dashed curve illustrates the attenuation of iron nuclei [30].

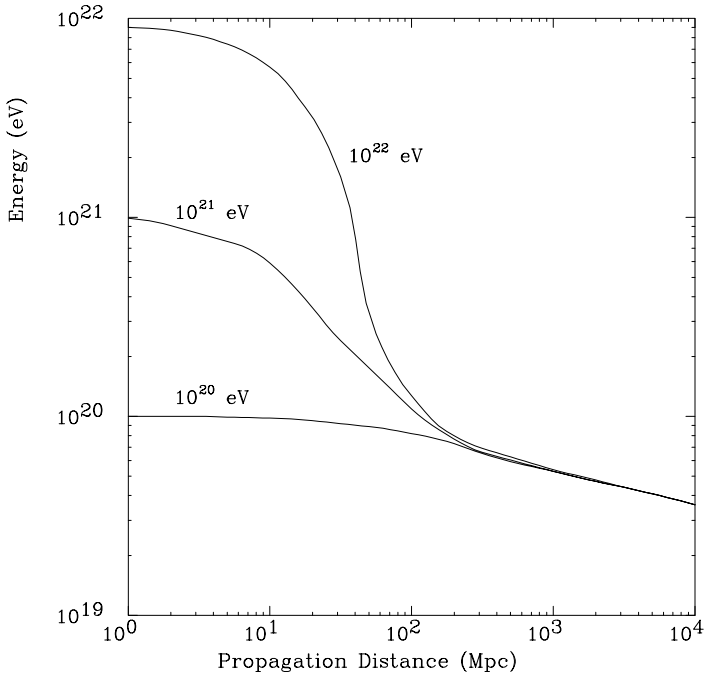

Figure 2.5: Energy of a proton as a function of propagation distance through the 2.7 K cosmic background radiation for various initial energies [31, 32].

energy. This is illustrated for protons in Figure 2.5 [31, 32]. This figure shows how, as described above, the energy of a proton effectively degrades due to successive photopion interactions with the CMBR. The GZK limit is evident, i.e., the flux of protons observed with energies exceeding about 10^{20} eV, regardless of their initial energy, is sharply reduced if they have traveled more than 100 Mpc.

Stated more generally, the attenuation length of protons and nuclei in the microwave background depends strongly on energy, especially in the region of the threshold for photopion production. As a result, the *observed* shape of the spectrum will depend strongly on the distribution in time and space of the sources, as well as the initial energy spectrum of the particles. Some examples are illustrated in Figures 2.6 and 2.7 [33]. Figure 2.6 shows the energy spectrum observed at earth if protons originate from a single source with an initial differential energy spectrum proportional to E^{-2}. The observed spectrum is very sensitive to the distance of the source, showing a sharp GZK cutoff when the source exceeds a distance corresponding to a redshift[2] of $z = 0.01$ (≈ 50 Mpc).

Figure 2.7 gives the observed spectrum for a different situation, where there are many sources of cosmic rays, distributed uniformly in space ("cosmologically"). Again, the spectrum is complex and sensitive to details of the production process. The five curves correspond to models in which cosmic ray production is increasingly important in the past and for which the cut-off effect is therefore more severe. For example, the curve labeled 1 corresponds to a

[2]Redshift z is the fractional wavelength change in radiation from distant sources due to the expansion of the universe. To first order, z is proportional to the source distance: d $\approx zc/H \approx z \times 5000$ Mpc, where H is the Hubble constant.

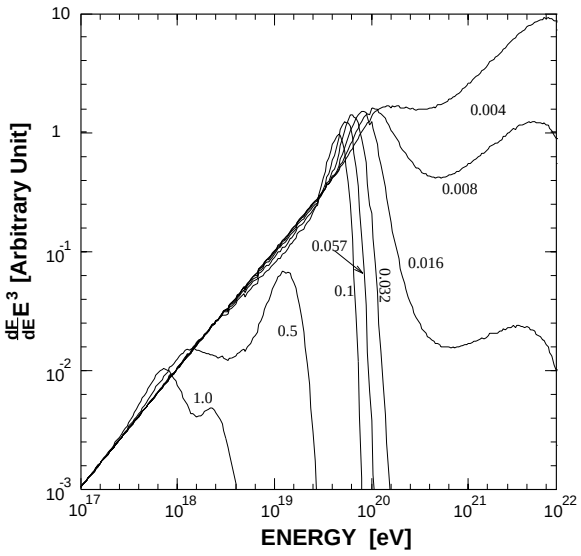

Figure 2.6: The observed energy spectra assuming a single source of protons with an E^{-2} injection spectra[33]. Spectra are shown for various fixed source distances corresponding to redshifts z = 0.004 to 1 (i.e., from about 2 Mpc to 5 Gpc).

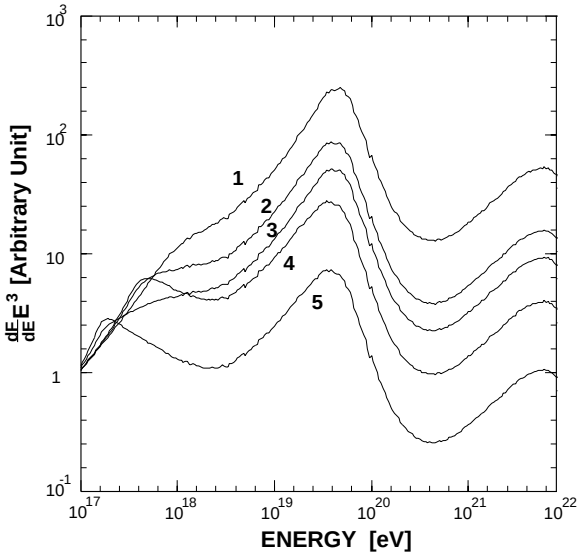

Figure 2.7: Observed spectra from several cosmological distributions of sources [33], leading to a strong cut-off below 10^{20} eV. The five curves correspond to models in which the cosmic ray production is increasingly important in the past and for which the cut-off effect is therefore more severe.

uniform distribution of sources up to a red-shift of $z = 2$ but with no cosmological evolution. Curve 5 is a model in which the sources extend back to red-shift $z = 4$ and the sources are assumed to be significantly more active in the past than at present.

Figure 2.7 also indicates another general feature of the GZK effect, that of a slight recovery of spectra if they extend to energies of $10^{21} - 10^{22}$ eV or higher. The interactions which cause losses are primarily resonance phenomena (e.g., Δ^+ production). The "dip" in the spectra seen in Fig. 2.7 near 10^{21} eV reflects this. Most of the acceleration models described earlier are clearly unable to generate particles at such extreme energy, but some of the exotic scenarios predict fluxes possibly observable in very large detectors such as the Auger Observatory. There has also been recent work which points out that the energy of the GZK cutoff might be significantly higher if the cosmic rays are light ($\sim$ 1 GeV) SUSY particles[34], because the interaction threshold is higher. Such speculation is interesting in light of the fact that cosmic rays are now known to exist above 10^{20} eV.

It is not easy to fit the experimental observations with combinations of the spectra of Figure 2.6. These data are discussed more fully in the next chapter, but note, for example, that a source sufficiently nearby to account for two events observed above 2×10^{20} eV tends to yield more particles than are actually observed just below this energy. The data may actually indicate an anomalously low flux or "gap" in the spectrum around 10^{20} eV, perhaps indicating a transition where one source's spectrum overtakes another. Unfortunately, existing detectors have insufficient exposure for this feature around 10^{20} eV to be considered to be statistically

significant.

Thus, particles with $E > 10^{20}$ eV must come from relatively nearby (Figure 2.5). Because extragalactic fields are expected to be weak (probably $< 10^{-9}$ G [35]), the particle trajectories will be only slightly deflected. We can expect to do particle astronomy with these particles. A major goal of the Auger Project is to accumulate enough particles above 10^{20} eV to identify source locations based upon arrival directions.

The observation of extragalactic sources of ultra high energy cosmic rays by the Auger Project will establish important constraints on the poorly known structure and strength of extragalactic magnetic fields. The study of the spectrum, composition, and directional distribution of cosmic rays with energies above $\sim 10^{19}$ eV will probe extragalactic magnetic fields below the present observational upper limit of $\sim 10^{-9}$ G [35]. The angular distribution of the arrival directions of charged cosmic rays with respect to their source(s) conveys information about extragalactic fields. In addition, ultra high energy photons interact with magnetic fields, and so will exhibit an alteration in their observed spectrum around $\sim 10^{19}$ eV for extragalactic magnetic fields in the range $10^{-9} - 10^{-11}$ G [36]. Probing extragalactic fields will help answer the question of how they originated and whether the galactic magnetic field is purely a primordial relic or was dynamically enhanced from a much smaller cosmological seed field. Either case will have important consequences which extend from understanding galaxy formation to the study of processes in the early universe (e.g., phase transitions) which generate magnetic fields.

2.3 Recent theoretical work

We have mentioned above general principles of and constraints on mechanisms of particle acceleration. Spurred by recent detection of cosmic ray events apparently exceeding the GZK cutoff, there has been much recent work on detailed models. This section highlights some of this work, emphasizing how different models may have signatures discernable by the Auger Observatory. Three kinds of models are considered:

- Gradual acceleration in large objects, such as radio galaxies;
- Acceleration in catastrophic events, e.g. in association with gamma-ray bursts;
- Exotic sources, e.g. topological defects or monopoles

There are also some remarks on the inevitable production of astrophysical neutrinos associated with the cosmic rays.

None of the models described here can be considered complete. We conclude the section with comments on the considerable work which remains, with emphasis on the need for more and better data at the highest energies. The Auger Project aims to provide the data which is necessary for further progress.

2.3.1 Shock acceleration in extended sources

In the preceding section, broad arguments were presented which showed that if the highest energy cosmic rays were produced through Fermi acceleration associated with strong shock waves, then the most likely sources were extragalactic. That the highest energy particles require extragalactic sources has long been recognized [37]. There are a variety of scenarios for accelerating particles in large-scale astrophysical structures. The following are examples which have been recently investigated in detail:

- Large scale structure formation in the universe could lead to very large scale shocks and associated particle acceleration [38].
- Shocks in the accretion flows in clusters of galaxies, possibly already observed in an absorption feature in the Perseus cluster. If the magnetic fields are strong enough, particles can be accelerated to high energy [39].
- Collisions of galaxies, fairly common in dense clusters, are expected to generate shock waves [26].
- Shocks in the lobes at the ends of the high speed jets observed in some powerful radio galaxies may be sites of particle acceleration. Some are sufficiently nearby to supply events above 10^{20} eV [40].

Detailed discussion of all of these mechanisms is beyond the scope of this Report. However, as an illustration of the issues involved, we discuss the last scenario in more detail.

It is natural to consider radio galaxy jets as possible accelerators since they are among the few structures in the cosmos with sufficient size and magnetic field strength to support shock acceleration to 10^{20} eV (recall Figure 2.2). Many objects with strong radio jets have been observed to be emitters of GeV gamma-rays by the Compton Gamma Ray Observatory[41]. There is also convincing evidence that the gamma ray spectrum from two AGNs (Markarian 421 and 501, whose jets are pointing toward earth) continues into the TeV energy range [42]. These high energy gamma rays are produced by electrons or protons of still higher energy. In either case, they indicate the tremendous energy flow in the jets.

Localized regions of especially intense radio emission, so-called "hot spots", are sometimes seen within the lobes at the ends of the jets of high power radio galaxies. These features are usually interpreted as large scale plasma shock waves in the jets, possibly weakly relativistic [40, 43]. Objects which exhibit hot spots are a small sub-class of all radio sources called Fanaroff-Riley Class II (FR-II) galaxies.

It is important to recognize that models of acceleration to extreme energy will also have consequences at much lower energy. Particles will "react" on fields which have been influenced by the shocks responsible for the highest energies. When constructing models to explain 10^{20} eV particles, one must simultaneously respect constraints imposed by other observations. Consider, for example, that it has been empirically known that certain otherwise

very different objects have some puzzlingly similar properties of their optical radiation. Radio quasars with strong red optical emission, the jets in M87, and optical emission from FR-II radio galaxy hot spots all share two common properties: i) The emission is polarized, and is therefore almost certainly synchrotron emission from very energetic electrons/positrons and ii) the emission cuts off sharply near 3×10^{14} Hz. The generality of such a finding in both compact and extended objects, and sources as different as the M87 jet and radio galaxy hot spots, suggest rather simple underlying physics. A comprehensive model, addressing a very wide range of energy, is required.

In 1987, Biermann and Strittmatter proposed [40] that Fermi acceleration of protons at shock fronts could provide a basis for a physical interpretation of the preceding observations. As described earlier, protons are accelerated near shock waves until they reach a sufficiently high energy where losses in their interaction with the ambient magnetic and photon fields compensate for any further gains. The highest energy protons in turn initiate turbulence in the thermal plasma, which can be described as a superposition of component "waves" whose wave-numbers have a power-law distribution. The turbulence spectrum power-law can be related to the synchrotron emission spectrum integrated over the emission region. Indeed the same standard power-law is found in almost all systems, including the solar wind and in the interstellar medium. In this resulting wave field, electrons are also accelerated by the shock wave. The maximum synchrotron emission frequency is nearly independent of the magnetic field strength, depending weakly on the ratio of the energy density of photon and magnetic fields, and strongly on the shock velocity. The highest emission frequency possible in the rest frame of the shock is approximately 2×10^{15} Hz, assuming a rather simple shock geometry and non-relativistic flow. Recent optical observations in fact support such a number for the cut-off frequency of the synchrotron emission [44] .

A key feature of the model is that the acceleration to the highest energies occurs far from the central engine where the intense radiation would cause severe energy losses to cosmic ray particles. An important result was the prediction that radio galaxy hot spots could accelerate protons to 10^{21} eV [45, 46]. Indeed, the model *required* that protons be accelerated to extreme energy in order to explain the lower energy observations.

A relativistic flow could obviously increase both the maximum cut-off frequency and the maximum proton energy. The ultimate power source for the plasma shock waves in the jets of strong radio sources is the compact object at the center. One can scale the properties of radio jets and hot spots with the power of the central engine and estimate the maximum proton energy possible in any of the known radio galaxies. The maximum energy derived from this limiting argument is about 4×10^{21} eV [47].

Romero and coworkers [48] have also recently employed the "hot-spot" model to the nearby radio source Cen-A, predicting that it is capable of accelerating protons to a maximum energy of 2×10^{21} eV. If this analysis is correct, then because Cen-A is extremely close (3.5 Mpc), it would surely have been "seen" as a point-source had there been any cosmic ray experiments in the Southern Hemisphere with the collecting power and angular resolution enjoyed by the Northern Hemisphere's Akeno/AGASA or Haverah Park arrays.

If powerful radio galaxies are in fact the source of extremely energetic cosmic rays, then certain signatures should be evident:

- The arrival directions of individual events above 10^{20} eV — which are, it is supposed, only weakly deflected by intergalactic magnetic fields — should cluster about the direction of nearby strong radio galaxies, especially FR-II galaxies or those with highly asymmetric structures.

- The distribution of arrival directions of events above a few times 10^{19} eV should exhibit anistropy which increases with energy. The preferred directions should correlate with the distribution of nearby strong radio galaxies. These galaxies tend to lie along a broad swath of the sky known as the "supergalactic plane".

- Radio galaxy sources of the events above 10^{20} eV should also produce an excess of particles of somewhat lower energy from those same general directions.

- The cosmic rays are almost certainly protons or perhaps gamma-rays, since heavier nuclei are unlikely to survive transport from the central AGN through to the hot spots at the end of the jets.

The directions of extremely energetic cosmic rays events have been studied to see if they correlate with any known objects. There are interesting hints:

- The two highest energy events (a 3×10^{20} eV event from the Fly's Eye, and the 2×10^{20} eV event from Akeno) appear to come from the general locations of FR-II galaxies, probably nearby ones[49]. The likelihood of a random association of the event directions with FR-II galaxies is small, since there are very few such sources in the sky within modest distances.

- Evidence for a directional clustering along the supergalactic plane has recently been published, for cosmic rays whose energies exceed 4×10^{19} eV[50, 51, 52]. The statistical significance of these observations is rather small, however.

Pending the collection and analysis of a far larger body of data, it is premature to draw strong conclusions from either of the above observations. Each will be discussed more fully in the next chapter (Sections 3.3.1 and 3.3.2).

The association of event directions with the supergalactic plane is an example of a more general situation discussed by Berezinsky et al.[27] in which there is an excess of sources in the local supercluster. The prediction of clustering in the supergalactic plane would hold for any mechanism associated with mass concentrations in our part of the Universe.

The shape of the cosmic ray energy spectrum near the expected cut-off may tell us about the relative density enhancement of nearby sources. This is particularly true if all sources are of a similar nature. However, if it is impossible to distinguish one source from another based on the arrival directions or if different source types are involved, the situation

is considerably more complicated. Even if the sources are of a similar type, such as the lobes of radio galaxies, each system would be expected to have somewhat different parameters and correspondingly different values of E_{max}, some above and some below the GZK cut-off.

Better angular resolution, a sensitivity to the nuclear type of the primary cosmic ray particle, and many more events above 10^{20} eV are needed to resolve the situation. The Auger Project aims to meet these needs.

2.3.2 Association with gamma-ray bursts

Gamma-ray bursts (GRBs) are observed (by satellites) as short, intense bursts of keV-GeV gamma rays. Despite hundreds having been detected (at a rate of about one per day), their origin and nature are unknown. It is possible that GRBs are indicators of some catastrophic event during which cosmic ray particles are shock-accelerated to extreme energies.

Recent observations give increasing evidence that the sources of GRBs are distributed throughout the entire universe (a "cosmological" origin)[53]. If GRBs are indeed so very far away then they must be very powerful. It is interesting that the power needed to account for the energy flux of the highest energy cosmic rays is comparable to the average rate (over volume and time) at which energy is emitted as γ-rays by GRBs in the cosmological scenario. These facts invite the suggestion that GRBs and high-energy cosmic rays have a common origin.

Aspects of the data (such as millisecond variability, a hard spectrum sometimes extending to GeV energies, etc.) impose strong constraints on the physical conditions in the γ-ray emitting region[54]. It has been suggested that protons may be Fermi accelerated in this region to $10^{20} - 10^{21}$ eV [55, 56]. Waxman has argued[57] that the cosmic ray spectrum above 10^{19} eV is consistent with a cosmological distribution of sources of protons having a power law generation spectrum $dN/dE \propto E^{-x}$, with $x = 2.3 \pm 0.5$ (consistent with the universal value characteristic of Fermi acceleration by strong shocks).

An essential ingredient of a cosmological GRB model for high energy cosmic rays is a time delay due to inter-galactic magnetic fields (IGMF). Consider the two most energetic cosmic ray events yet recorded, from the Fly's Eye and the Akeno experiments. The energy of the most energetic cosmic ray detected by the Fly's Eye experiment was 3×10^{20} eV, and that of the most energetic AGASA event was 2×10^{20} eV. As was shown in Figure 2.5, the distance such energetic particles could travel before becoming victims of the GZK cutoff is < 100 Mpc. The arrival directions of the two events are sufficiently separated that we will assume that they did not originate from the same GRB event within such a distance. Furthermore, the two events were recorded within 26 months of each other. Assuming GRBs have a cosmological origin, the rate of relevant "nearby" GRBs is rather small. Based on the GRB observations from BATSE, there is about one GRB per 50 years in the field of view of the cosmic ray experiments and within 100 Mpc [58]. The observed short time difference between the Fly's Eye and AGASA events can be reconciled with the typical rate of GRBs if the dispersion in the arrival times of protons produced in a single burst is longer than a time on the order of the average time difference between GRBs. Therefore, 10^{20}eV protons produced in a distant

GRB must arrive at earth dispersed in time over ≥ 50 years. Dispersions of this magnitude are quite plausible, produced by the combined effects of deflection by random magnetic fields and energy dispersion of the particles, provided that the IGMF is $\geq 10^{-12}$ G ([55, 59]; see also Figure 2.9 later in this chapter).

An arrival time dispersion exceeding 50 yr implies that no correlation between the arrival directions of cosmic rays and gamma-rays should be expected on a much smaller time scale, unless the GRBs are very nearby. Since the BATSE observations started only about 5 years ago, it is not possible to conduct an extensive search for correlations between extreme-energy cosmic ray events and older GRBs. Nevertheless, it was pointed out [60], that the arrival direction error box of the most energetic Fly's Eye event is consistent (within errors) with that of the strongest GRB recorded in the first two BATSE catalogues (still among the highest 1% of all BATSE events collected). Similarly, the most energetic AGASA event is within 5° of another strong GRB. There are many BATSE events, so it is not unlikely to find one near either the Fly's Eye or Akeno events. It is nevertheless noteworthy that these GRBs are so strong.

Clearly, many more cosmic ray events at the highest energies must be collected in order to test the hypothesis of an association with GRBs. If the possible correlation between the arrival directions of either the Fly's Eye or Akeno event with strong GRBs is confirmed (by observing new events above 2×10^{20} eV to be correlated with GRBs on time scales of a year or so), this would imply that the rate per unit volume of nearby GRB events is much higher than that expected from a cosmological distribution. Such a finding would strongly suggest that the (common) sources of GRBs and of high energy cosmic rays are Galactic [61, 59].

If the highest energy cosmic rays are associated with nearby GRBs (e.g., in the Galactic halo), one expects: (i) new $> 10^{20}$ eV events to be correlated with GRBs; (ii) no GZK cutoff; (iii) highly isotropic cosmic ray distribution, due to the observed isotropy of GRBs. If, on the other hand, the high energy cosmic rays are associated with cosmological GRBs, one expects a GZK cutoff, and, if GRB sources are associated with luminous matter, anisotropy related to the large-scale structure of the local (< 100Mpc) universe, since cosmic rays cannot travel far.

In addition to the latter signatures, which are common to any model with cosmological distribution of cosmic ray sources, the cosmological GRB model for high energy cosmic rays predicts several unique signatures [62]. The energy dependent delays in the cosmic ray arrival times, induced by the IGMF, result in individual cosmic ray sources having narrow observed spectra, since at any given time only those cosmic rays having a fixed time delay are observed. Thus, the brightest cosmic ray sources may be different at different energies.

Another possible signature is a delayed flux of moderately high energy photons[59]. The energy lost by the cosmic rays as they propagate and interact with the microwave background is transformed by cascading into secondary GeV-TeV photons. A significant fraction of these photons can arrive with delays much smaller than the cosmic ray delay if much of inter-galactic space is occupied by large-scale magnetic "voids", regions of size $\sim$ 5Mpc or larger and field weaker than 10^{-15}G. Such voids might be expected, for example, in models where a weak primordial field is amplified in shocked, turbulent regions of the intergalactic

medium during the formation of large-scale structure. For a field strength $\sim 4 \times 10^{-11}$G in the high field regions, the value required to account for observed Galactic fields if the IGMF were frozen in the protogalactic plasma, the delay of cosmic rays produced by a burst at a distance of 100Mpc is $\sim$ 100yr, and the fluence of secondary photons above 10 GeV on hour–day time scales is $I(> E) \sim 10^{-6} E_{\rm TeV}^{-1} {\rm cm}^{-2}$. This fluence is close to the detection threshold of current high-energy γ-ray experiments. It will be described later how the Auger Observatory ought to be sensitive as well, by observing enhanced individual detector singles rates over the entire array.

If the suggested association of the highest energy cosmic rays with cosmological GRBs is true, then the expected signatures should be identifiable once the number of events observed above 10^{19}eV is increased by a factor of several tens [57, 62]. This would require ~ 50 observation-years with existing experiments, but only a few years operation of the Auger Observatory. Confirming an association of the highest energy cosmic rays with GRBs (either Galactic or cosmological) would have profound influence on our understanding of both phenomena, and would also provide information on the poorly known IGMF.

2.3.3 Exotic sources

The difficulties so far encountered in modelling the production of extremely high energy cosmic rays arise from the need to identify an astrophysical environment capable of raising low energy particles to extreme energy. In contrast to "bottom-up" acceleration of charged particles in active galactic nuclei or other astronomical objects, there could be a "top-down" (TD) mechanism where the (charged and/or neutral) primaries are produced at extreme energies in the first place.

Topological Defects

One example invokes the decay of supermassive "X" particles. These particles may be radiated from *topological defects* formed during phase transitions as the early universe cooled, a product of spontaneous symmetry breaking implicit in some Grand Unified Theories (GUTs)[63, 64]. Relic topological defects, such as ordinary and superconducting cosmic strings, domain walls, and magnetic monopoles, are relatively stable topologically, but can release part of their energy in the form of X particles, if they collapse or annihilate.

The X particles, with typical GUT scale masses on the order of 10^{24} eV, subsequently decay into leptons and quarks. The strongly interacting quarks fragment into jets of hadrons resulting in typically $10^4 - 10^5$ mesons and baryons. Certain TD scenarios (e.g., annihilation of bound states of magnetic monopoles) are capable of producing extremely energetic cosmic rays at the observed level [65]. There is, then, the exciting possibility of connecting cosmic rays to new fundamental physics. Since the predicted density of topological defects is very model dependent [66], measurements of the highest energy cosmic rays may impose tight constraints on the theory.

The shapes of the nucleon and γ-ray spectra produced in TD models are expected to be

universal (i.e., independent of the any specific TD scenario) above 10^{20} eV, depending only on the physics of X particle decay. This is because at these energies, nucleons and γ-rays have attenuation lengths in the cosmic microwave background radiation (CMBR) which are small compared to the Hubble scale (the "red shift limit" in Fig. 2.4). Cosmological evolutionary effects which depend on the specific TD model are therefore negligible. Since the resulting spectra tend to be considerably harder than acceleration spectra, TD mechanisms could contribute to the flux dominantly above $\simeq 10^{20}$ eV, but negligibly in the range 10^{14} eV – 10^{19} eV.

TD models of the origin of the highest energy cosmic rays are subject to a variety of constraints which are mostly of cosmological nature. For example, the predicted neutrino flux and the γ-ray flux below $\sim 10^{14}$ eV depend on the energy release integrated over redshift and thus on the specific TD model. Compared to acceleration scenarios, this energy release can be substantial, especially at high redshifts where there is no contribution from conventional sources like galaxies. Electromagnetic energy injected into the universe above the pair production threshold on the CMBR is recycled into a generic cascade spectrum below this threshold on a time scale short compared to one Hubble time. This can have several potentially observable effects, such as modified light element abundances due to ^{4}He photodisintegration, distortions of the CMBR, and neutrino fluxes at earth. Comparison with observational data already rules out a certain class of TD models related to superconducting cosmic strings [67].

If a TD model is to explain the origin of the highest energy cosmic rays, its predicted spectrum must be normalized to account for the events observed above 10^{20} eV without violating any observational flux measurements and limits at higher and lower energies. Observational data on the universal γ-ray background in the 100 MeV region [68, 69, 70] to which the generic cascade spectrum would contribute directly turn out to play an important role in that respect. Since especially the extreme energy γ-ray flux depends sensitively on some astrophysical parameters like the extragalactic magnetic field, a reliable calculation of the predicted spectral shapes requires numerical methods [71]. Interestingly, in the case of TD scenarios with uniform injection (as expected, for example, in case of monopole annihilation [65]) the resulting constraints are somewhat modified compared to earlier analytical estimates [67]. For certain extragalactic magnetic fields, X particle masses as high as 10^{25} eV are quite viable [72]. An earlier claim that TD models might already be ruled out altogether [29] can only be substantiated for the case of discrete sources with monoenergetic injection [71], but there is still concern that the predicted gamma ray emission at 3×10^{20} eV and above is too large.

Since it is currently not possible to determine unambiguously the composition of extremely energetic cosmic rays, the normalization procedure has to involve the sum of the nucleon and γ-ray fluxes. This, in turn, predicts the spectrum and composition at other energies and offers certain signatures typical for the TD scenario: a hard TD component could produce a pronounced recovery in the form of a flattening beyond the GZK cutoff. This might become an important signature for TD scenarios in case a considerable rate of superhigh energy events above 2×10^{20} eV is found and if the "gap" in the cosmic ray spectrum between these events and the lower energy data should prove to be real [73]. Acceleration

models cannot account for a gap due to their softer spectra. Furthermore, within TD scenarios, the flux above 10^{20} eV would be dominated by γ-rays, as opposed to the case of an acceleration origin [74]. In addition, an isotropic γ-ray component at the 10% level of the total flux at 10^{19} eV would hint at the presence of a TD mechanism and a large scale magnetic field weaker than about 10^{-11}G [72]. Another indicator for new physics would be the detection of a substantial neutrino flux above 10^{18} eV. Combined with bounds on contributions to the low energy γ-ray background, its magnitude would yield important information on the decay mechanism operating in a possible TD scenario [75].

In summary, the signature of TD models is a very hard cosmic ray spectrum ($\sim E^{-1.5}$) dominated by neutrinos, gamma rays, and protons. The proton component comprises only a few percent of the total flux. The majority of the particles are light and uncharged, and would presumably include any exotic varieties that might exist (e.g., photinos). Overall, the spectrum extends to extraordinarily high energy, near the X-particle mass of perhaps 10^{24} eV. The hardness and high energy of the spectrum may provide events whose energies are well beyond the GZK cutoff.

These distinctive characteristics arise because the particles are produced in the decay of massive X bosons. Observation of such a spectrum would be extremely interesting because theories with a real grand unification simple group will have such heavy particles, while most classes of string theories do not. For them, $SU(3) \times SU(2) \times U(1)$ directly unify at the string scale, without a larger group entering. String theories can produce topological defects[76], but the mechanisms for producing cosmic rays are different. Cosmic ray data that implied the existence of heavy bosons would have a major impact on efforts to formulate a fundamental theory.

Confirmation of the existence of an "exotic" component of cosmic rays, such as produced by topological defects, would potentially provide insight into the conditions in the early universe, as well as into particle physics beyond the "Standard Model".

Magnetic monopoles

Another idea utilizing topological defects is one where relic magnetic monopoles themselves constitute the highest energy primary cosmic rays. This possibility was first raised in 1960 by Porter[77]. We discuss here a more recent investigation of this idea by Kephart and Weiler[78].

As in the earlier discussion of GRBs, the consideration of relic monopoles as an explanation of cosmic rays is motivated by two interesting facts:

- The observed cosmic ray flux above 10^{20} eV is similar to the theoretically allowed *Parker bound*[79] (the maximum flux of relic monopoles which would not destroy the observed interstellar magnetic field).
- Under reasonable assumptions about field strengths and field coherence lengths, Dirac monopoles can be accelerated to energies beyond 10^{20} eV.

If the highest energy cosmic rays are indeed magnetic monopoles, they must be relativistic to transfer enough energy to the atmosphere to initiate air showers and thus they must have masses less than 10^{19} eV. Because there is a monotonic relationship between the allowed monopole flux and mass in cosmological models of monopole origin, this provides another limit on the density of monopoles which is consistent with the Parker bound. It may also lead to an energy threshold for the initiation of observable air showers, an important prediction if indeed the apparent "gap" in the energy spectrum of cosmic rays around 10^{20} eV is confirmed by further data.

The monopole hypothesis has observational consequences. One is that energetic monopoles may be expected to be distributed preferentially in the direction of the local galactic magnetic field. Another may be that air showers produced by monopoles have distinctive characteristics.

Detailed modelling of the interactions of magnetic monopoles in the upper atmosphere has not been carried out to date. The electromagnetic component is not difficult to calculate and should resemble the interactions of a particle of charge 137/2, but the hadronic component is likely to be complicated. For monopoles of mass greater than 10^{15} eV, the energy loss per scatter is expected to be rather small, leading to a shower that is initiated over a longer distance, and the scattering angle per collision is expected to be larger, scaling as $1/\gamma$. It is not yet known whether a monopole can produce an air shower which would mimic what is expected for a hadron primary and in particular the rather "normal" looking cascade development which was observed directly with the Fly's Eye (see the next chapter, section 3.2.2).

The detectors of the Auger Observatory are designed to be sensitive to air shower structure in order to study effects related to the nuclear composition of the primary particles.

2.3.4 Astrophysical Neutrinos

A common feature of most of the models of cosmic ray sources discussed above is the production of extremely high energy neutrinos. The detection of neutrino fluxes would provide valuable additional experimental signatures to distinguish different models. The Auger Observatory will be able to detect and identify extremely energetic neutrinos, if their flux is high enough.

Neutrinos provide a unique opportunity to explore regions of the Universe that are otherwise obscured by either large depths of matter or by the attenuating effects of intense radiation fields (recall Figure 2.4). Neutrinos are uncharged and have a very small interaction cross section, so they emerge unscathed from even the most active locations. Neutrinos are undeflected and virtually unattenuated while traversing very long cosmic trajectories, thus providing a way to study the possible sites of cosmic ray origin in a manner complementary to that using other particles.

The recent discoveries of GeV and TeV $\gamma-$ray sources seemingly necessitates the production of neutrinos within AGN, radiogalaxies, blazars, and quasars [80]. Charged pions are

produced in these astrophysical beam dumps and decay into neutrinos. The mechanism of the GZK cutoff itself is also a source of high energy neutrinos through the $\Delta^+ \to \pi^+ + ... \to \nu + ...$ decay sequence[81]. Neutrinos are also one of the main expected byproducts of two possible cosmic ray production mechanisms described above: the decay of topological defects [63, 64], and GRB's [82].

In summary, all proposed cosmic sources of extremely energetic cosmic rays seem inevitably to produce energetic neutrinos in numbers possibly large enough to be observable. Their detection would provide independent support for these models. Moreover, the relative fluxes of neutrinos and cosmic rays should give extremely valuable information on the distance at which they are produced because of the difference in their interaction lengths in intergalactic space. The ability of the Auger Observatory to detect high energy cosmic neutrinos will be discussed in the next chapter.

2.3.5 Summary Comments on Source Models

Our survey of recent theoretical work has just shown several very interesting alternatives to the problem of the origin of the highest energy cosmic rays. All of these models begin to penetrate the fundamental mystery: how can such extraordinary energies be achieved? Yet none of the ideas is yet completely satisfactory. Here are some the important issues which need to be clarified:

- An approximately homogeneous distribution of radio galaxy sources predicts that the cosmic ray energy spectrum observed at earth will show the GZK cutoff. It would not permit many particles well above 10^{20} eV and yet there are now several such candidates observed. Are there too many?

- The GZK cutoff is avoided only if the sources are nearby. That is, all observed cosmic rays are *young*. For radio galaxy sources, a strong preponderance of such young particles might be plausible if we lived in a rich cluster, or if the radio sky were dominated by a single brilliant source. But neither is the case. There is no independent reason to suppose that there is such a strong local overdensity of radio galaxy sources.

- With the exception of radio galaxy hot spots, the cited models of shock acceleration in extended sources would appear to be too slow to work (recall Figure 2.3). The energy losses associated with interactions on the cosmic background radiation exceed the acceleration gains by the time the particles approach 10^{20} eV. Thus no particles exceeding about 10^{20} eV appear able to emerge from most sources.

- Likewise, GRB sources of cosmic rays, if they are distributed homogeneously throughout the universe, should exhibit the GZK cutoff. This or any homogeneous model is not viable if very many events are observed well above 10^{20} eV.

- Nearby GRB sources (i.e., in our Galaxy or its corona) would avoid the GZK cutoff, but no theory for acceleration to extreme energy has been proposed. It is certainly not expected in any of the popular models of Galactic GRBs involving neutron stars.

- Topological defect models predict a cosmic ray spectral *shape* similar to that which is being observed at the highest energies. However, its normalization is not calculated from first principles. When set to agree with the rate at which events above 10^{20} eV have been observed, it may predict too many particles at even higher energies. This possible conflict is very uncertain due to the lack of data at such high energy. However, this normalization may also have problems at lower energies. Some TD scenarios may be ruled out by measured upper limits on 100 MeV diffuse gamma-ray fluxes if the mean intergalactic field strength exceeds 10^{-11} G or if the TD annihilation rate evolved early in the universe as strongly as the theoretically favored time dependence (t^{-3}).

It is clear that the most important things needed to further our physical understanding are more, and better, data. An accurate, high-statistics measurement of the energy spectrum, arrival directions, and particle identity of the highest energy cosmic rays will be provided by the Auger Observatory's detectors. While these data may not conclusively establish any of the models as they now stand, it is an absolutely necessary part of the effort to achieve the final goal of understanding the origin of the highest energy cosmic rays.

2.4 Observational capabilities needed for the Auger Observatory

As discussed above, models of acceleration and propagation do not satisfactorily account for all the observations of cosmic rays at the highest energies. This is an assurance that either new fundamental physics or unanticipated astrophysics will result from solving this mystery. With only incremental increases in detector aperture, however, the discoveries will be a long time coming. The promise of new physics is ample motivation to increase the collecting power now by a large factor. The largest current surface array (AGASA) has an area of 100 km^2. The Auger Project will achieve a 60-fold increase in collecting power with an area of 6000 km^2. Complete sky coverage with fairly uniform celestial exposure is essential for a sensitive search for arrival direction anisotropy. The detector must also measure cosmic ray directions, energies, and identify the types of particles accurately.

2.4.1 Composition resolution.

The mass composition of cosmic rays is a powerful constraint on theories. Highly charged nuclei are easier to accelerate to high energies than protons, although they are susceptible to photodisintegration at the source and during propagation. Gamma-rays and neutrinos are potentially unique signatures of exotic models. The mass composition should be determined at all energies. It is especially important to identify the particle type(s) arriving with energies above the expected GZK cut-off (which occurs at different energies for protons and heavy nuclei). The goal is to achieve sufficient energy and mass resolution to resolve the situation above 10^{19} eV in which all of the following effects might be manifest:

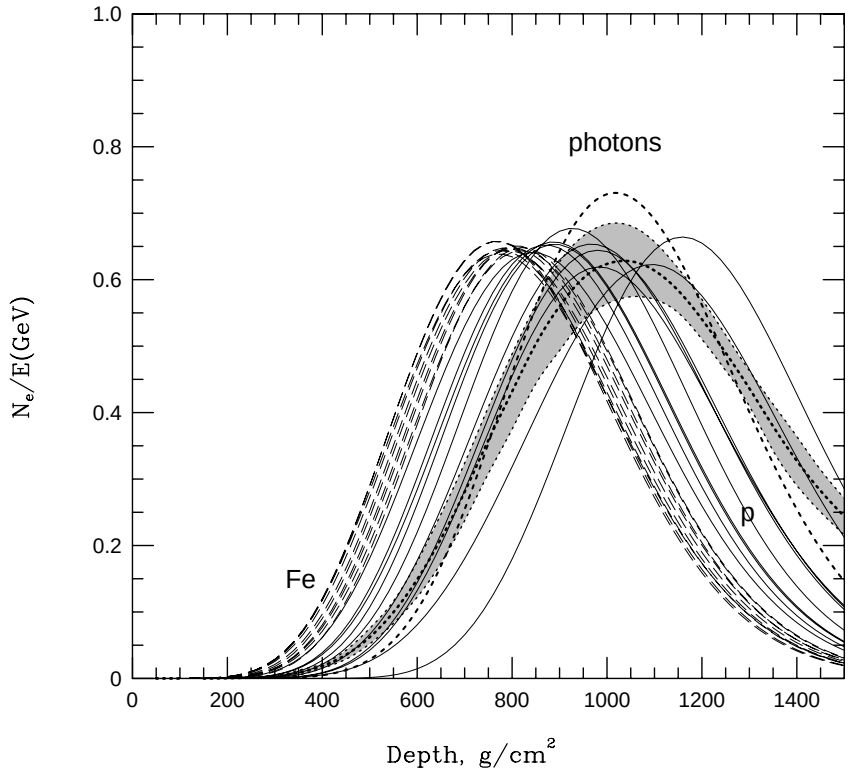

Figure 2.8: Longitudinal development of air showers with energies near 10^{20} eV produced by protons, iron nuclei, or photons. Ten showers each are individually shown for protons (thin solid lines) and iron nuclei (thin dashed lines). The calculation for photons was performed two ways: the shaded band includes the LPM effect and interactions with the geomagnetic field, while the thick dashed is simple electromagnetic cascading only.

- A GZK cut-off.
- Events beyond the GZK cut-off, contributed by nearby sources. The energy spectrum might exhibit a characteristic dip-bump structure if there are new and/or exotic source for the highest energy particles.
- Energy-dependent composition associated with the upper limiting energies of different contributing sources.
- Energy-dependent composition associated with differential attenuation in the intergalactic medium.

To accomplish this goal it will be necessary to be able to distinguish among the three major groups of potential primaries: primordial nuclei (protons and helium), products of stellar nucleosynthesis (carbon and heavier), and photons (expected in some models of exotic sources).

One way to distinguish primary particle types is by measuring the way the extensive air shower develops. Figure 2.8 shows a comparison of the longitudinal shower profiles for

different types of primaries, from a one dimensional monte-carlo simulation. The curves show the growth and attenuation of air showers in terms of the number of electrons N_e present at various atmospheric depths.

Average shower development curves for photon induced air showers are also shown in Figure 2.8. The banded curve for photons includes the cascading in the geomagnetic field as well as the LPM effect[3]. The thick dashed line shows the profile that would be expected for a simple (Bethe-Heitler) electromagnetic cascade only.

It must be noted that current uncertainty in knowledge of hadronic interactions at such high energy leads to uncertainties in the expected X_{max} – the depth in the atmosphere where the shower reaches the maximum number of particles – for iron and proton showers, although their *difference* is not strongly model dependent[84]. The calculated profiles for protons (and to a lesser extent heavy nuclei) also have inherent systematic uncertainties as a consequence of the need to extrapolate hadronic interactions many orders of magnitude beyond accelerator energies. The main effect of these uncertainties would be to shift the entire profile to the right or left by amounts possibly as much as 100 g/cm^2, since only the first few interactions occur at such unexplored energy regimes.

The calculation used to estimate the air shower development curves in Figure 2.8 was a simplified one-dimensional simulation. A more sophisticated and detailed simulation (described in Chapter 4) confirms the features shown here, predicting the mean X_{max} difference between iron and proton showers is about 70 g/cm^2.

The numbers of muons and electrons in air showers also differ between events initiated by protons, gamma rays, and heavier nuclei. Gamma-ray showers have far fewer muons than hadron showers. Heavy nuclei at the same total energy as a proton will yield showers with more muons. These effects are discussed in more detail in Chapter 4 (section 4.2.3), where simulation of air shower physics is discussed. The Auger Observatory's ground detectors will have good ability to distinguish primary mass groups based on muon and electron measurements. When combined with measurements of the shower longitudinal development by the fluorescence detector of Auger, the power of the experiment is further increased.

2.4.2 Energy resolution

An accurate measurement of the spectrum requires both adequate statistics and good energy resolution. Energy measurement errors distort a steeply falling spectrum because each energy bin gains many more mismeasured showers from lower energies than it does from higher energy. It will be shown later (Chapter 5, section 5.2.5) that structures in the shape of the cosmic ray energy spectrum (like the GZK cutoff) can be clearly resolved if the experimental $\delta E/E$ resolution is less than about 20%.

[3]The Landau-Pomeranchuk-Migdal (LPM) effect is a quantum mechanical alteration of electromagnetic showers at very high energy. Roughly put, bremsstrahlung has a "formation length", governed by the uncertainty principle, which grows with the electron's energy. Radiation begins to be suppressed when this length becomes comparable to the distance between scatterings[83].

By designing the detector to have good mass resolution, it will necessarily have good energy resolution. The Auger Observatory fluorescence detector should measure the atmospheric depth of shower maximum (X_{max}) to an accuracy of 20 g/cm^2 (as mentioned above, the mean X_{max} for iron showers is about 70 g/cm^2 higher in the atmosphere than that from protons of equal energy). As will be seen in a later chapter, a 20 g/cm^2 X_{max} resolution implies that the integral of the longitudinal profile (i.e., the total energy) can be fitted with less than 10% uncertainty. Systematic uncertainties from modeling the atmosphere may also be present. Similarly, the ground array should have sensitivity to composition by measuring separately the muon and electromagnetic ($e + \gamma$) particle fluxes. By achieving adequate accuracy in the muon/electromagnetic ratio, particle density measurements will necessarily provide good energy resolution.

2.4.3 Arrival direction resolution

Detector requirements for anisotropy studies depend on the particular energy range of interest. For energies above 10^{20} eV, magnetic deflection of protons by Galactic or extragalactic magnetic fields is expected to be so small that detector angular resolution is an issue. For charged particles of lower energy, point source resolution is limited by magnetic scattering – detector angular resolution is important only if there is a flux of neutral particles. A very large exposure is then needed in order to detect any anisotropy or clustering of arrival directions. At the detector's energy threshold, scattering by magnetic fields may be so severe that the distribution of arrival directions differs from isotropy in only a subtle way: in addition to large numbers of events, a fairly uniform exposure will be vital for sensitive detection of such patterns.

For a source at distance L_{kpc}, the trajectory of a charged particle in a uniform magnetic field is curved such that the observed angular deviation of its arrival direction with respect to the straight line of sight to its source is:

$$\theta \approx 0.3^{\circ} \frac{L_{kpc} Z B_{\mu G}}{E_{20}} = 0.3^{\circ} \frac{L_{Mpc} Z B_{nG}}{E_{20}}, \tag{2.3}$$

if the deflection is reasonably small (i.e., $\sin\theta \approx \theta$). This expression is an immediate result of Equation 2.2 using $L = R\theta$. The particle energy E_{20} is in units of 10^{20} eV, the field strength B transverse to the particle motion is in μG when L is in kpc or nG when L is in Mpc. The former case is typical of Galactic dimensions and fields, the latter for extragalactic paths. Z is the charge of the particle in units of e.

The left side of Figure 2.9 displays the observed angular deflection from Eq. 2.3 as a function of energy for protons. One line is calculated for a source distance of 0.5 kpc and an intervening transverse magnetic field of 2 μG (typical of the Galaxy's disk thickness and field intensity). The same line in the figure happens also to pertain to a distance of 1 Mpc through a transverse extragalactic field of 1 nG.

The assumption of a value of order nG for extragalactic magnetic fields is not supported by observations (see the discussion at the end of the first section of this chapter). Intergalactic

field strengths and coherence lengths are not well established, but it is plausible to assume that fields have coherent directions on scales of about 1 Mpc. A long trajectory is multiply deflected, each "scatter" contributing an independent angular deviation whose magnitude is roughly given by Eq. 2.3. The number of scatterings is given by the path length divided by a *step size*. The step size l is taken here as the coherence length, so the number of scatterings is equivalent to the source distance in units of Mpc. The average total angular deviation of the arrival direction from the line of sight to the source can then be approximated as $\sqrt{L_{Mpc}}$ times the angular deviation over 1 Mpc. The left side of Figure 2.9 exhibits the result for a linear distance to the source of 30 Mpc (a typical distance to other galaxies in our local cluster). These assumptions about extragalactic field strength and coherence length are not verifiable, but they provide a specific model for examining the energy dependence of magnetic deflections.

Magnetic bending of particle trajectories causes them to arrive later than photons emitted simultaneously from the same source. For a simple circular arc path, the expected delay is given by

$$\triangle t \;\approx\; 0.012\ yrs\ \times L^3_{kpc} Z^2 B^2_{\mu G}/E^2_{20} \;=\; 12.0\ yrs\ \times L^3_{Mpc} Z^2 B^2_{nG}/E^2_{20},$$

with L the straight-line distance to the source. For multiple scattering with step size l_{Mpc}, the delay is

$$\triangle t \;\approx\; 6.0\ yrs\ \times L^2_{Mpc} l_{Mpc} Z^2 B^2_{nG}/E^2_{20}.$$

The right side of Figure 2.9 shows the expected proton time delay as a function of energy for Galactic and extragalactic path lengths. The Galactic path is taken, as before, to be a circular arc originating from a source 0.5 kpc distant and $B = 2\mu$G. The extragalactic path length is again taken for a source distance of 30 Mpc, $B = 1$ nG, and with a step size $l_{Mpc} = 1$. It is notable that the time delays expected for extragalactic sources can be very large, preventing the association of charged cosmic ray arrival times with astrophysical events at the source observed in photons or other neutral particles.

The search for point sources or an anisotropic cosmic ray arrival direction distribution will have energy dependent requirements. We discuss below three energy ranges pertinent to Auger observations.

$\mathbf{E > 10^{20}}$ eV

The estimated angular deflection of a 10^{20} eV proton over Galactic distances is 0.3°, as shown in Figure 2.9. If extragalactic deflections are negligible, then charged particle astronomy is certainly possible and a detector angular resolution which is small compared to 0.3° would be desirable in order to locate the sources as precisely as possible. However, extragalactic deflections are likely to exceed the Galactic deflection, even though pion photoproduction limits the path lengths to about 50 Mpc. According to the model of multiple scattering outlined above, the arrival directions from a single source would be dispersed by $(\sqrt{50}) \times 0.3° = 2.1°$. It is important that the detector angular resolution be better than this in order to take full advantage of the high magnetic rigidity. Based on the present uncertain intensity

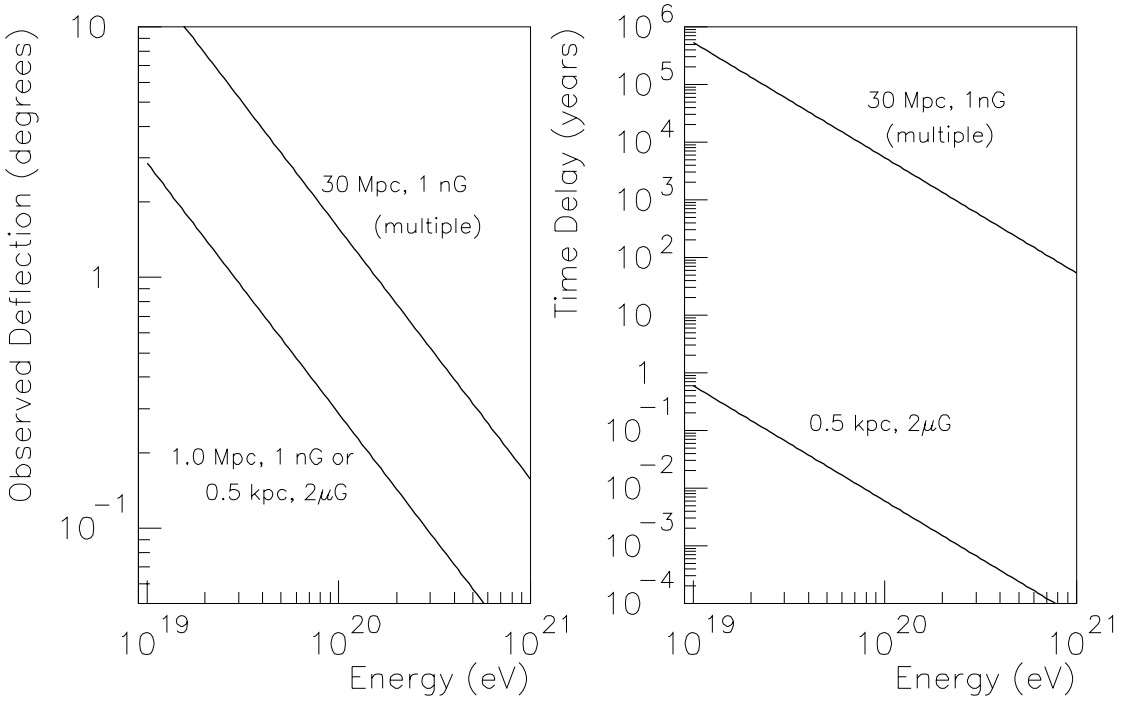

Figure 2.9: Magnetic bending of protons. On the left, the observed deflection from a straight-line path for several cases: travel through the Galactic disk or a path of 1 Mpc through extragalactic space, and multiple scattering over 30 Mpc (assuming a field coherence length of 1 Mpc). On the right side, the time delay relative to a straight line trajectory for two of these cases.

determinations, the Auger Observatory may detect about 180 such particles in three years. It may then be obvious if the number of contributing sources is much less than 180, based on the presence of tight clusters. Sensitivity to "repeaters" depends on angular resolution. If the angular resolution is limited only by this 2.1° magnetic deflection, the expected number of error circles overlapping by chance if randomly distributed on the sky would be about 20. If degraded further by a 3° detector angular resolution, for example, the number of chance overlaps would be about 70. Detector resolution better than 2° is desirable in case extragalactic magnetic deflections are less than estimated here and in case there is a flux of neutrons (whose decay length $\gamma c\tau$ is about 1 Mpc at 10^{20} eV) or γ-rays.

$\mathbf{E} > 4 \times 10^{19}$ eV

Recent analysis of Haverah Park [50] and AGASA data [52] suggests that there is an excess of arrival directions associated with the "supergalactic plane"[4]. The observed anisotropy begins to be seen at about 4×10^{19} eV. If confirmed, this is an exciting result because it would verify a variety of expectations. The first expectation is that particles of such high energy should be magnetically rigid enough to point back to their sources with only small deflection, even for rather large source distances. Another expectation is that particles at these energies have not traveled more than a few hundred Mpc, since attenuation from the GZK effect would become severe (recall Figure 2.4). Within that nearby volume of space, the mass density of the universe is biased toward the supergalactic plane. Any theory of energetic particle production would predict the source locations to be correlated with the mass distribution. The importance for this discussion is the observational evidence that the cosmic ray population above 4×10^{19} eV is not isotropic, implying that the shower directions do indeed carry information about source locations.

In three years of running, the Auger Observatory will collect more than 1000 showers above 4×10^{19} eV with approximately uniform sky exposure. Figure 2.9 gave the expected angular deflection for protons as 0.7° at 4×10^{19} eV . Assuming a typical source distance of 200 Mpc,then the multiply-scattered arrival directions should be distributed about the source directions by $(\sqrt{200}) \times 0.7^\circ = 10^\circ$. Unless there are very many sources, clusters from individual sources should be evident. Figure 2.10 shows a simulation of the Auger sky at energies above 4×10^{19} eV after 3 years if all the cosmic rays come from 15 sources of approximately equal flux. Each source is smeared by sampling its arrival directions from a 10° Gaussian. The source locations are easily seen by eye and their coordinates can be localized to within $10^\circ/\sqrt{N}$ for N events from each. A realistic map would have a variety of source fluxes and magnetic dispersions. Higher flux and smaller dispersion makes a discrete source easier to detect.

Note that the orientations of the arrival directions around the sources in Figure 2.10 were simulated by *uniformly* placing them around the source direction. Each cluster thus has a circular appearance on the sky map. In reality the clusters will have more complex shapes which depend upon the magnetic fields and the energy spectrum of the particles[86].

[4]Recall that the supergalactic plane is a swath of sky which includes the locations of most of the nearest galaxies. The evidence for an excess of events from this direction is discussed in Section 3.3.1.

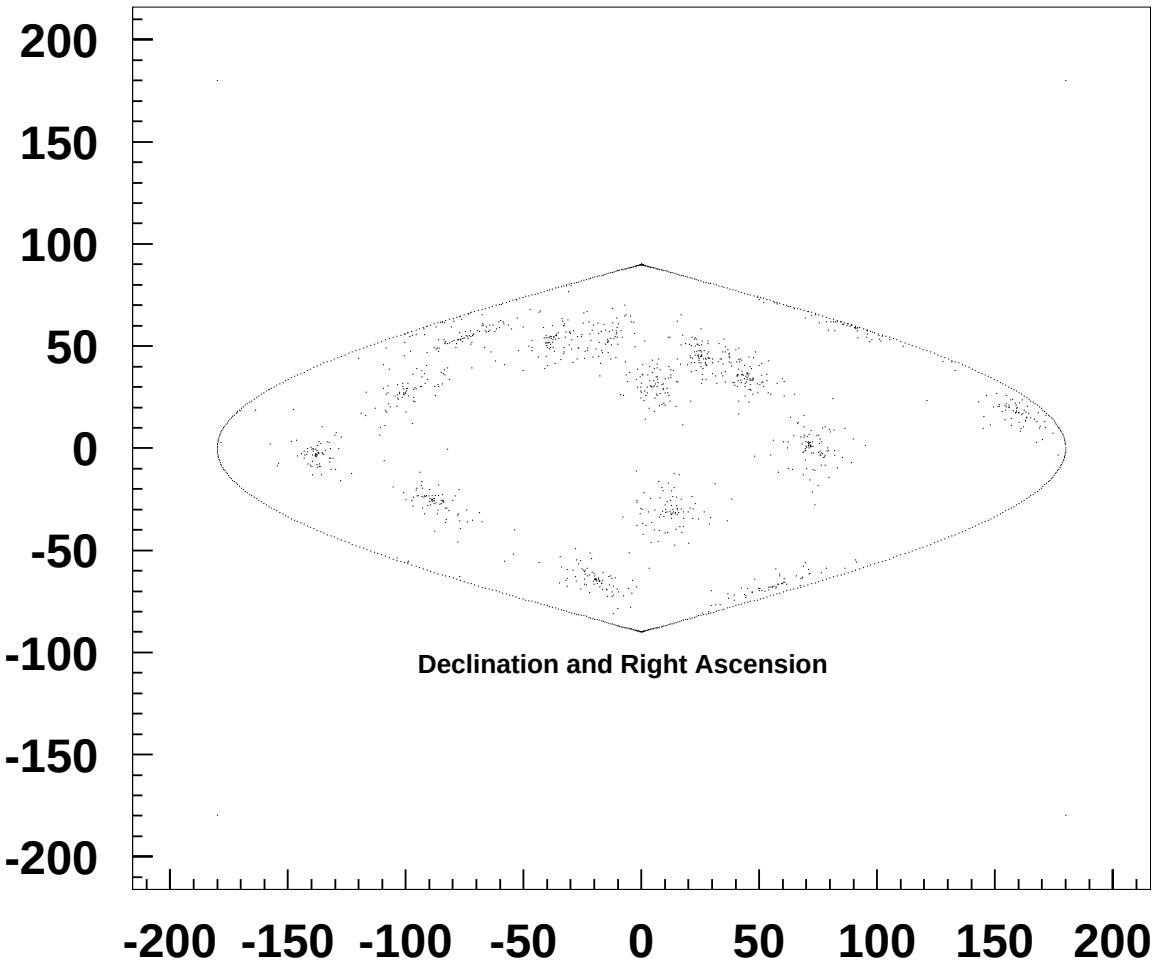

Figure 2.10: Simulation of the Auger sky for showers with energy greater than 4×10^{19} eV after 3 years (1165 showers expected). Positions for 15 point sources of approximately equal flux were chosen randomly. Each simulated source is smeared by sampling a Gaussian of 10° width.

For example, the arrival directions might form thin arcs on the map, passing through the source locations. In any case there will likely be a correlation of displacement with energy. Thus, anisotropy analysis benefits greatly from both good direction reconstruction accuracy and good energy resolution.

E $> 10^{19}$ **eV**

The anisotropy analysis is expected to be more complicated using all the Auger Observatory showers above 10^{19} eV. The problem is not lack of statistics, as 18,000 showers should be collected in three years. The difficulty is due in part to the fact that the GZK effect does not significantly attenuate these particles, and so there is no effective distance limit imposed on the possible source locations. Thus, the detected particles may have suffered magnetic scrambling over cosmological times, perhaps having originated from a source distribution which reflects the large scale homogeneity of the universe. There may also be a

non-negligible contribution from our Galaxy at 10^{19} eV. If the cosmic rays of galactic origin are all heavy nuclei at this energy (due to preferential acceleration and confinement), an analysis excluding small mass primaries could reveal a pattern produced by sources in the galactic disk compounded by propagation through the Galaxy's magnetic field.

A sensitive anisotropy analysis is greatly facilitated by uniform sky exposure. This is a primary reason for building identical detectors in both the northern and southern hemispheres. Previous experiments have had highly non-uniform exposure, including large areas with no exposure whatsoever. A search for arrival direction anisotropies under those conditions is extremely difficult, and analysis by spherical harmonics is not feasible. Even the simplest search for a dipole harmonic cannot be conclusive. This point was emphasized in the 1980s when an apparent negative gradient was reported in galactic latitude [87, 88, 89]. The initial interpretation was that the intensity of cosmic rays is greater from southern latitudes than from the galactic northern hemisphere. Wolfendale and Wdowczyk [90] pointed out, however, that for a detector with a north-dominated exposure, such a gradient could also be construed as evidence for an excess from galactic *equatorial* regions, without any actual north-south asymmetry in the cosmic ray intensity. With poor exposure to south galactic latitudes, two radically different interpretations were viable.

Identical installations in both the northern and southern hemispheres will ensure that the Auger Observatory has nearly uniform exposure to the entire sky. A small exposure dependence on declination will remain, but it is well known and can easily be corrected for. The Auger Observatory will be the first opportunity to study cosmic ray arrival directions over the full celestial sphere with good efficiency.

2.4.4 Neutrino Astronomy

It was noted in the last section that most proposed cosmic sources of extremely energetic cosmic rays seem surely to lead to associated neutrino fluxes. Their detection would provide independent and complementary information to discriminate between models. Here, we describe the sensitivity of a general purpose cosmic ray detector to extremely energetic neutrinos. The main method to differentiate neutrino-induced air showers from ordinary cosmic rays is to use their very low interaction cross section to advantage: neutrinos will produce *horizontal* air showers ("HAS") over the Auger Observatory far more easily than ordinary hadronic cosmic rays can.

The first requirement of any neutrino detector is a large target mass. Several experiments are currently under development to instrument large volumes of water or ice with photomultipliers and detect the Čerenkov light from neutrino interactions [80]. These detectors sense the Čerenkov light produced either by muons (from charged current ν_μ interactions) or electromagnetic cascades (ν_e interactions). Theoretical estimates of TeV and PeV neutrino fluxes from quasars and radiogalaxies have motivated recent interest in 1 km^3 H_2O detectors.

It has also been known for a long time that deeply penetrating high energy particles such as muons and neutrinos initiate horizontal air showers that can be detected at ground level [91]. Since the mean free path for muons and neutrinos in the atmosphere is larger than

the whole atmospheric depth, they have roughly equal probability to interact at any point in the atmosphere. The rate of air showers due to the hadronic cosmic rays decreases very rapidly with zenith angle as the atmospheric depth rises from about 1000 g/cm^2 vertically to nearly 4×10^4 g/cm^2 horizontally. The electromagnetic component of air showers is absorbed well before reaching the Earth's surface, leaving only muons for events at sufficiently large zenith angles. An air shower array that is sensitive to muons, like that planned for Auger, is then also sensitive to penetrating neutrino events.

Large zenith angle events were first observed in the 1960's [92] for moderately large air showers (10^3 to 10^5 particles). They have been interpreted as electromagnetic showers induced by hard bremsstrahlung events from the conventional atmospheric muon flux (π and K decays) alone[93]. Such events, whether induced by muons or neutrinos, have inspired a range of theoretical and experimental interest. It has been recently stressed that HAS of higher energy can be related to the charm production cross section [94] and to composition [95]. The power of the HAS technique is evident in recent results which ruled out one prediction of neutrino fluxes from AGN [96]. For all these reasons, HAS are currently being studied by several particle array groups [97], [98].

To estimate the sensitivity of a ground array to neutrino induced events, it is useful to compute the effective *volume* of the detector. This measure is most easily compared among different kinds of experiments. The effective volume for neutrino detection through HAS is calculated as the product of its projected area and the range of depths within which the shower must originate in order to trigger the device. It is necessary at this point to assume some detector details, in accord with the proposed configuration for the Auger detectors which is described later in this Report. We shall assume that the ground array consists of individual stations, spaced 1.5 km from one another, each registering a "hit" if the air shower particle density exceeds some assumed value ρ_e^{th}. The boundary of the array encloses a total area of about 3000 km^2. A calculation has been done using parametrizations of particle lateral distributions for showers, and demanding that three stations in a row have electron number density above ρ_e^{th} [99]. The results are illustrated in Figure 2.11.

Note that the effective volume of a device like that described here exceeds 10^4 km^3 of air for large showers. Despite the low density of air, the effective target mass is comparable to a 1 km^3 water detector. Lower energy showers may also be detected if they are aligned with rows of detectors in the array, but the effective volume is greatly reduced.

Also note that we have not included an optical detector in the computation leading to the results in Figure 2.11. An air fluorescence device, like the one described later in this Report, gives additional information which may increase the acceptance of the experiment and will certainly improve the reconstruction of HAS over that which could be done by a ground array alone.

When the effective volume as computed above is convolved with predictions of the neutrino flux from topological defect decay[64, 100] or from the GZK cutoff reactions[81], it reveals that measurable rates are within reach of the Auger Observatory. In Table 2.1 we give the yearly event rates expected under two extreme extrapolations of the neutrino cross section to these energies: the parton distributions of Martin, Stirling, and Roberts are denoted MRS

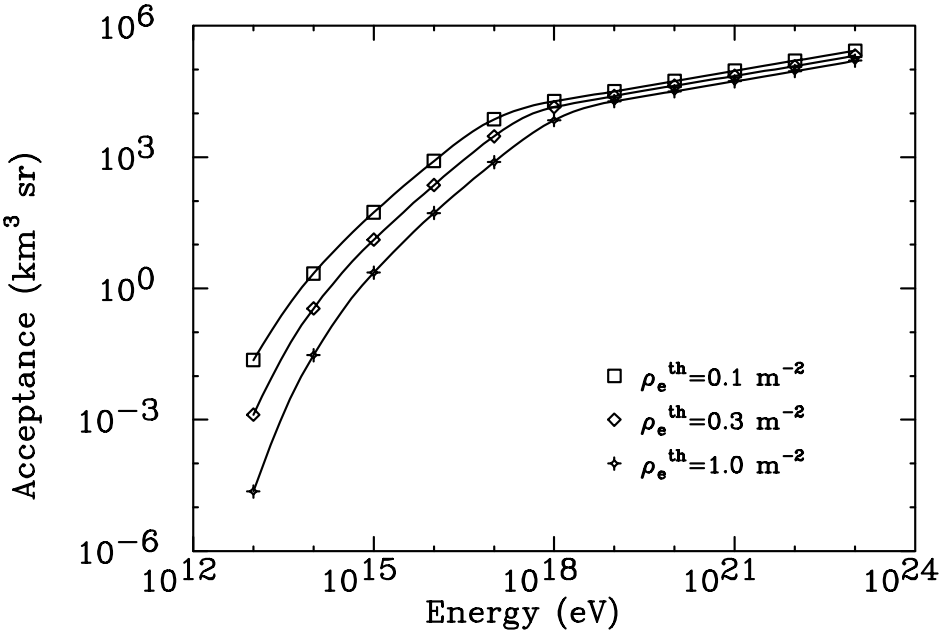

Figure 2.11: Acceptance of a large ground array to neutrino induced air showers, expressed in terms of its effective volume (km^3 of air) and field of view (steradians). The configuration and triggering of a ground array has been modeled as described in the text. Results of separate calculations assuming three different thresholds for individual surface stations to participate in a trigger are indicated.

Table 2.1: Neutrino event rates (per year)

ρ_e^{th} (m^{-2})	MRS	GRV
	Interactions with Cosmic Microwave Background	
1	1	0.5
0.1	3	1
	Topological Defects	
1	27	8
0.1	51	17

[101], those of Glück, Reya, and Vogt as GRV [102]. (A recent analysis suggests that the true value of the cross section is likely close to that found using the MRS assumptions[103]). It can be seen that the results are not very sensitive to the assumed threshold ρ_e^{th} of individual detectors because most of the events are due to very large showers.

The size of the Auger Observatory, which will use both a fluorescence detector and a ground array, provide a unique oportunity to study HAS of greater energy than before. The sensitivity is optimal for showers of energy above 10^{19} eV, as is the case for ground detectors measuring more vertical events. This is one of the most interesting energy ranges for neutrino astronomy. Sources include the GZK cutoff interactions, from which neutrinos are produced as byproducts. Others may include the large neutrino fluxes expected from the decays of topological defects.

The interaction cross section of the photinos or the lightest SUSY particles is expected to be comparable to that of neutrinos. If the highest energy cosmic rays are produced by topological defects, and supersymmetric ideas are correct, some of any observed HAS should be photinos. Demonstrating this would not be easy, but they would appear as a component of the data with anomalous interaction cross sections.